Eur. Phys. J. B **6**, 295–299 (1998)

THE EUROPEAN PHYSICAL JOURNAL B

Raman and infrared spectroscopical investigation of the optical vibrational modes in GaSb/AlSb superlattices

A. Milekhin[1,2,a], T. Werninghaus[2], D.R.T. Zahn[2], Yu. Yanovskii[1], V. Preobrazhenskii[1], B. Semyagin[1], and A. Gutakovskii[1]

[1] Institute of Semiconductor Physics, 630090, Novosibirsk, Russia
[2] Institut für Physik, Technische Universität Chemnitz, 09107 Chemnitz, Germany

Received: 11 May 1998 / Accepted: 21 July 1998

Abstract. The vibrational spectrum of ultra-thin layer GaSb/AlSb superlattices was investigated in detail by infrared (IR) and Raman spectroscopies. The effect of confinement of the transverse and longitudinal optical phonons in both types of the layers was studied. The dispersions of optical phonons of the GaSb and the AlSb obtained from the analysis of the Raman and IR spectra are in a good accordance with the theoretical data and results of neutron scattering experiments. First- and second-order Raman spectroscopy indicates the presence of intermixture of atoms at the interfaces in the GaSb/AlSb superlattices.

PACS. 63.20.Dj Phonon states and bands, normal modes, and phonon dispersion – 78.30.Fs III-V and II-VI semiconductors

1 Introduction

The vibrational properties of semiconductor superlattices (SLs), particularly of those GaAs/AlAs, have been extensively investigated by Raman and infrared spectroscopies during the past decade [1–4]. Considerable theoretical and experimental effort has been devoted to the confinement of the optical phonons in the GaAs/AlAs SLs with ultra-thin layers [5,6]. In contrast to the nearly-lattice-matched GaAs/AlAs system the GaSb/AlSb SLs are classified as SLs with strained layers because of the significant mismatch of the lattice constants of GaSb and AlSb (0.65%). These structures attract much attention due to their possible application in laser diodes [7]. However, only few papers concerning the study of the vibrational spectrum of the GaSb/AlSb SLs have been published [8–10].

As in case of the GaAs/AlAs superlattices the cationic masses in GaSb and AlSb are significantly different. This causes the confinement of optical lattice vibrations in the corresponding layers and leads to a quantization of the phonon spectrum. The selection rules for the Raman and IR spectroscopy allow different phonon modes in SLs to be observed. Therefore, the combination of both experimental techniques provides the whole information on the vibrational spectrum of superlattices.

In this paper the vibrational spectrum of the short-period GaSb/AlSb SLs, where the effect of quantization of phonons should be taken into account, has been studied by means of the FTIR and Raman spectroscopies.

[a] e-mail: milekhin@physicus.physik.tu-chemnitz.de

2 Experimental details

The $(GaSb)_n/(AlSb)_n$ SLs with systematically varied layer thicknesses (n = 2, 4, 7, 10, 15 monolayers) were grown by MBE at a temperature of 470 °C on (100) oriented GaAs substrates. A GaAs buffer layer undoped or doped with Si atoms ($n_{Si} = 2 \times 10^{18}$ cm^{-3}) with a thickness of 1 μm grown on the substrate was covered by an AlSb layer with a thickness of 0.3 μm. The number of periods was 200 for n = 2, 100 for n = 4, 7 and 50 for n = 10, 15. The IR reflection spectra of the SLs were recorded using a FTIR spectrometer Bruker IFS-113v in the spectral range of the optical lattice vibrations of the GaSb and AlSb (200–400 cm^{-1}) at a temperature of T = 80 K. The resolution was 1 cm^{-1} over the whole spectral range. The number of scans was 2000. IR spectra using p-polarized light recorded at the off-normal incidence ($\theta \approx 70°$) were measured to analyze both the transverse optical (TO) and longitudinal optical (LO) vibrational modes [11].

The Raman scattering experiments were performed at T = 80 K using the 514.5 nm (2.41 eV) line of an Ar^+ laser with a power of 8 mW entering the sample surface. The scattered light was analyzed in backscattering geometry using a Dilor XY triple monochromator equipped with a CCD camera for multichannel detection. The scattering geometries employed were $z(xx)-z$ and $z(xy)-z$ with x, y and z parallel to the [100], [010] and [001] directions, respectively. The monochromator slits were set to a spectral resolution of 2.9 cm^{-1} controlled by the Rayleigh scattered laser light.

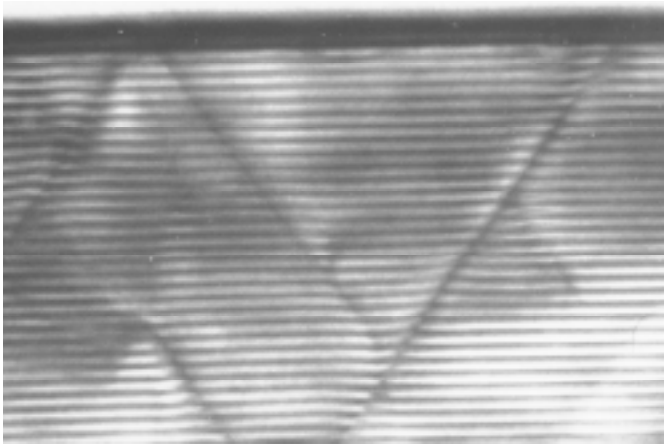

Fig. 1. Transmission electron microscopy photograph of the cross-sectional view of the $(GaSb)_{10}/(AlSb)_{10}$ SL. Light regions are the AlSb layers, dark regions are the GaSb layers.

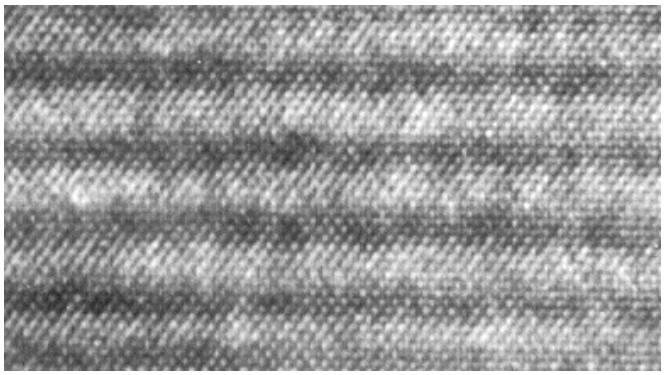

Fig. 2. HRTEM image of the $(GaSb)_4/(AlSb)_4$ SL. Light regions are the AlSb layers, dark regions are the GaSb layers.

3 Results and discussion

To validate the quality of the grown GaSb/AlSb SLs the cross-sectional transmission electron microscopy (TEM) experiments were performed. The TEM image of the $(GaSb)_{10}/(AlSb)_{10}$ SL shown in Figure 1 demonstrates a good crystalline quality of the sample. The strain in the SLs leads to appearance of the misfit dislocations. The high resolution TEM (HRTEM) experiments show that a crystalline quality, uniformity and the periodicity of the SL layers are conserved up to extremely thin SLs. Figure 2 shows that intermixing of atoms at the interface region in the $(GaSb)_4/(AlSb)_4$ SL of only 1–2 ML takes place.

The IR spectra of p-polarized reflectivity of the $(GaSb)_n/(AlSb)_n$ SLs with different thickness of layers measured in the spectral range of the GaSb optical phonons at oblique incidence of the light are presented in Figure 3. Features in the IR spectra marked by arrows are caused by the LO_1 and TO_1 vibrational modes localized in the GaSb layers. A shift of the fundamental LO and TO confined modes towards lower frequency with a decrease of the layer thickness is observed and reveals a strong

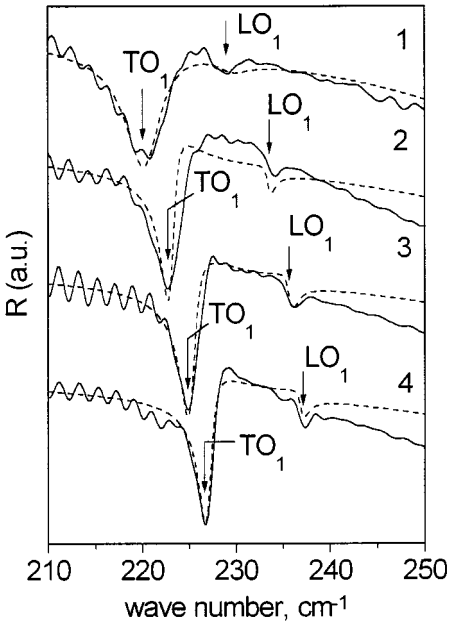

Fig. 3. IR reflection spectra of the $(GaSb)_n/(AlSb)_n$ superlattices in the spectral range of the optical phonons of the GaSb measured at off-normal incidence in the p-polarized light ($\theta \approx 70^\circ$) where $n = 2$ (curve 1), $n = 4$ (curve 2), $n = 7$ (curve 3), $n = 10$ (curve 4).

evidence of the confinement of the optical phonons in the GaSb layers of these SLs. Similar spectra were observed in the spectral range of optical phonons of AlSb.

In order to determine the frequency position of the confined modes a curve fitting procedure was employed. The theoretical spectra calculated by $E-H$ matrix method [12] are included in Figure 3 by the dashed lines. It was assumed that each layer of SL can be described by the following dielectric function:

$$\varepsilon_{1(2)} = \varepsilon_{\infty 1(2)} + \sum_i \frac{\Omega^2_{pi1(2)}}{\omega^2_{ti1(2)} - \omega^2 + i\omega\gamma_{i1(2)}} \qquad (1)$$

where $\varepsilon_{\infty 1(2)}$ is the high-frequency dielectric constant and $\omega_{ti1(2)}$, $\Omega_{pi1(2)}$, $\gamma_{i1(2)}$ are the frequency of the ith confined TO modes, the plasma frequency of the ith mode and the damping coefficient of ith mode, respectively. The index 1 corresponds to the GaSb layer and 2 to the AlSb layer. The best agreement of experimental and calculated spectra was obtained with the following parameters: $\varepsilon_s = 10.2$, $\varepsilon_{\infty 1} = 12.44$, $\varepsilon_{\infty 2} = 10.24$ are the high-frequency dielectric constants, $\gamma_s = 2$, $\gamma_{11} = \gamma_{12} = 1.5$ are the damping coefficients of the GaAs substrate and the first confined optical modes localized in the GaSb and AlSb layers, respectively.

In comparison to the IR experiments the Raman spectra produce more detailed information on the resonance vibrations in SLs. Due to the selection rules in the GaSb/AlSb SLs the odd and even LO confined modes are active in $z(xy)-z$ and $z(xx)-z$ scattering geometry, respectively. Figures 4a and 4b shows the first-order

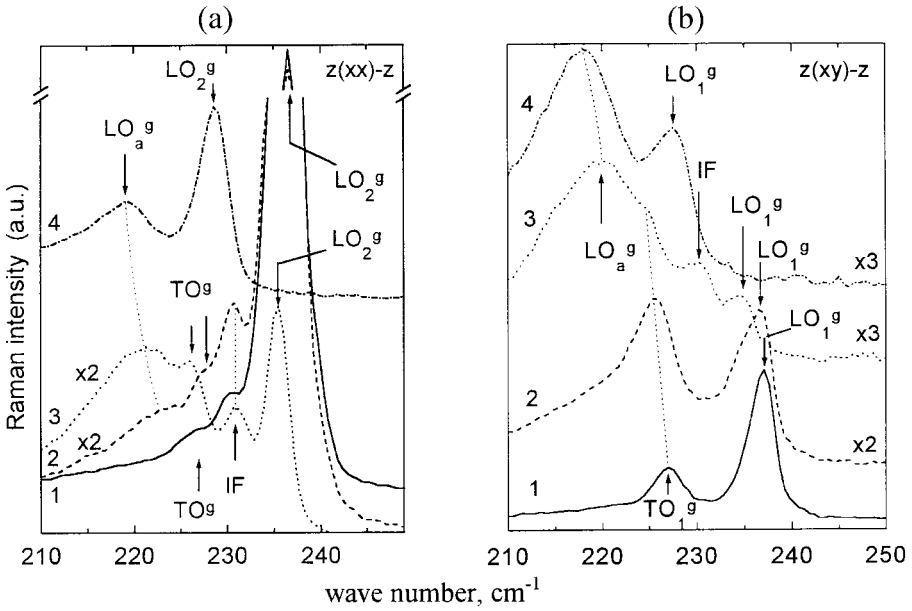

Fig. 4. Raman spectra of the $(GaSb)_n/(AlSb)_n$ superlattices in the spectral range of the optical phonons of the GaSb measured for $z(xx)-z$ (a) and $z(xy)-z$ (b) scattering where $n = 10$ (curve 1), $n = 7$ (curve 2), $n = 4$ (curve 3), $n = 2$ (curve 4).

Raman spectra of GaSb/AlSb SLs with different thickness of the layers measured for $z(xx)-z$ and $z(xy)-z$ scattering geometries in the spectral range of the optical phonons of GaSb. The Raman spectra reveal LO phonons and much weaker TO vibrational modes, forbidden in this configuration, confined within the GaSb layers. The assignment of the TO_1 confined modes in the Raman spectra measured for $z(xy)-z$ scattering geometries was performed due to a good coincidence of the frequency positions of the TO modes observed in the Raman and IR spectra. Here and further on the following notation is used. The subscripts 1 and 2 denote the quantum number of confined modes, the subscript a corresponds to the alloying mode and the superscripts g and a correspond to the GaSb- and AlSb-like phonons, respectively. To obtain the frequency position of vibrational modes a fitting of Raman spectra by Lorentzian peaks was performed.

With decreasing layer thickness of SLs the frequency position of the confined modes decreases. On the other hand, as it was shown earlier [13], the strain in $(GaSb)_n/(AlSb)_n$ SLs causes the shift of the confined modes of about $1 \div 2$ cm^{-1} for SL with $n > 7$ ML; in the SLs with a layer thickness less than 7 ML the strain is completely relaxed in the alloy interface region. In the ultra-thin layer SLs ($n < 10$ ML) the confined effect dominates and causes the decrease of the frequency position of the optical modes in these SLs.

In addition, broad features are observed in the spectral range below the TO phonons at a frequency ≈ 220 cm^{-1}. The intensity of these peaks increase with decreasing the SL periods. These vibrational modes were assigned to the LO GaSb-like modes (LO_a^g) originating from alloy interface layers. The thickness and the Ga content of these layers calculated with the use of frequencies of the allowing modes in the frame of next-nearest-neighbour linear chain model [3] are in good agreement with reference [13]. The weak features located between TO and LO modes of GaSb at the frequency ≈ 230 cm^{-1} were assigned to the SL interface (IF) modes [10].

The shift of the frequency position of vibrational modes as a function of layer thickness was observed also in the Raman spectra measured for $z(xx)-z$ and $z(xy)-z$ scattering geometries in the spectral range of the optical phonons of AlSb and presented in Figures 5a and 5b, respectively. The smaller downward shift of the LO_1^a and LO_2^a confined modes is explained by the negligible phonon dispersion of the LO phonons in AlSb in comparison with the dispersion of the LO phonons in GaSb. The features at the frequency 315 cm^{-1} and near 330 cm^{-1} are assigned to LO(Σ) phonon of AlSb [14] and interface modes [10], respectively. The vibrational modes placed near the LO and TO confined modes are related to the LO and TO AlSb-like modes from the alloy interface region (LO_a^a and TO_a^a modes).

The frequency positions of the confined modes obtained from the analysis of the IR and Raman spectra were used for the study of the phonon dispersion curves in GaSb and AlSb. Two treatments are used usually for determination of the dispersion curves from analysis of vibrational spectrum of SLs. The first one based on the three-dimensional lattice dynamic model (Ref. [15] and references therein) is more adequate but requires considerable calculations. The alternative approach assumes that optical vibrational modes are confined within the corresponding layers and their can be determined as follows

$$q_m = \frac{m\pi}{L_C a} \tag{2}$$

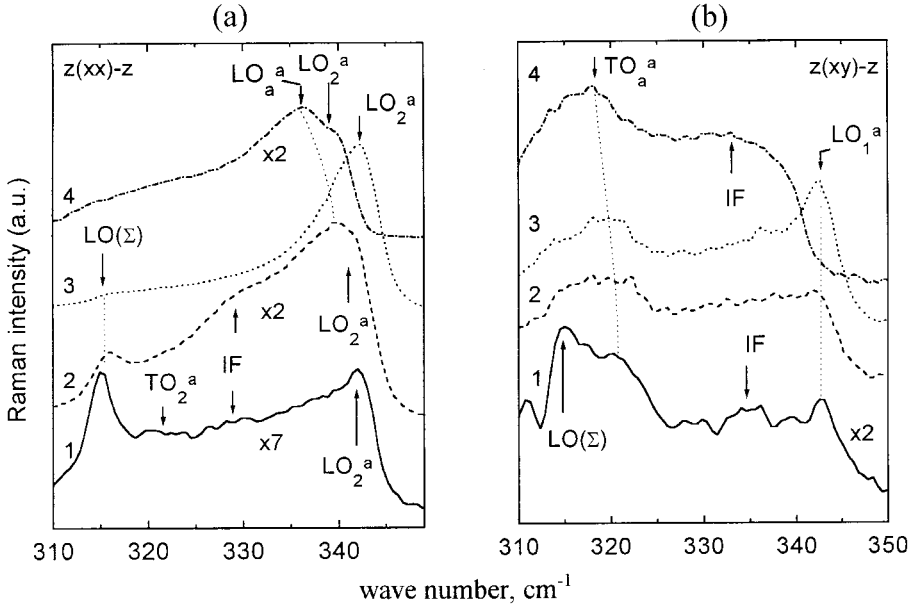

Fig. 5. Raman spectra of the $(GaSb)_n/(AlSb)_n$ superlattices in the spectral range of the optical phonons of the AlSb measured for $z(xx)-z$ (a) and $z(xy)-z$ (b) scattering where $n = 10$ (curve 1), $n = 7$ (curve 2), $n = 4$ (curve 3), $n = 2$ (curve 4).

where $L_C = n + \delta$ is the localization length, n is the number of monolayers in corresponding layer, m is the quantum number of confined mode, a is the lattice parameter and δ is a measure of a depth to which a confined mode penetrates into the neighbouring layers. Parameter δ reflects the nature of interfaces in interdiffused SLs. In this paper we use the second approximation taking $\delta = 1$ [10]. The quantum number and the frequency position of the confined modes allow the dispersion of the TO and LO phonons in GaSb and in AlSb to be obtained (Fig. 6). The dispersions deduced from the analysis of the IR and Raman spectra were compared with neutron [14,17] and previous Raman scattering data [9,16] and with calculated phonon dispersions [14,16]. As one can see from Figure 6 the experimental data are in good agreement with the theoretical calculations and the data obtained with another techniques. Due to tensile (compressive) stress in GaSb (AlSb) layers of the SLs we expect of systematical shift of the dispersion curves which does not exceed 2 cm^{-1}. The knowledge of dispersion is particularly important for TO phonons in the hygroscopic AlSb crystal, which is unstable in air, and for which there was no experimental data available up to now.

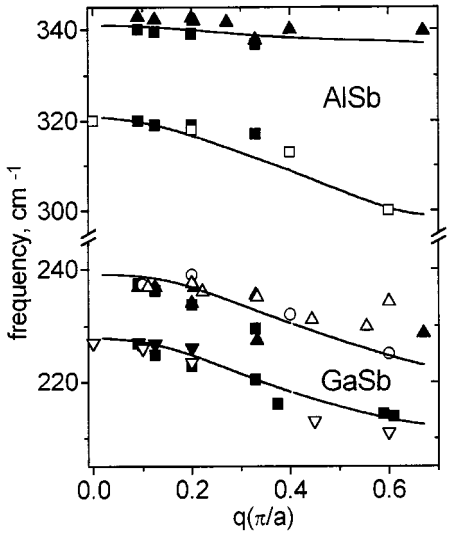

Fig. 6. Dispersion of the optical phonons of GaSb and AlSb. Our IR and Raman data are shown by the black solid squares and triangles, respectively, ○, □, ▽ are the neutron data, △ are Raman data from [9,14]. The theoretical dispersion curves are presented by solid lines.

The second-order Raman scattering spectra measured in $z(xx)-z$ and $z(xy)-z$ geometries are presented in Figures 7a and 7b, respectively. The second-order Raman modes revealed in the spectra were attributed to overtones and combinations following the previous theoretical and experimental results [14,18,19]. The strongest maxima in Figure 6a correspond to $2LO_2^g$ and $TO_2^g + LO_2^a$ modes. The frequency position of these modes is shifted with the decreasing thickness of SL layers in the low-frequency range according to the dispersion law of optical phonons in GaSb and AlSb. With decrease of the layer thickness new features assigned to the combination of alloying modes ($2LO_a^g$ and $LO_a^g + TO_a^a$) appear at frequencies ≈ 430 cm^{-1} and ≈ 535 cm^{-1}. The weak features at frequencies ≈ 425 cm^{-1} and ≈ 441 cm^{-1} are related to $2TO(X)^g$ and $2TO(L)^g$ modes measured earlier in bulk GaSb [18]. The same alloying modes are presented in the Raman spectra measured in $z(xy)-z$ geometry (Fig. 7b). Moreover, these spectra reveal a combination of the confined modes $2LO_1^g$ and $TO_1^g + LO_1^a$ which are shifted downward with decreasing layer thickness.

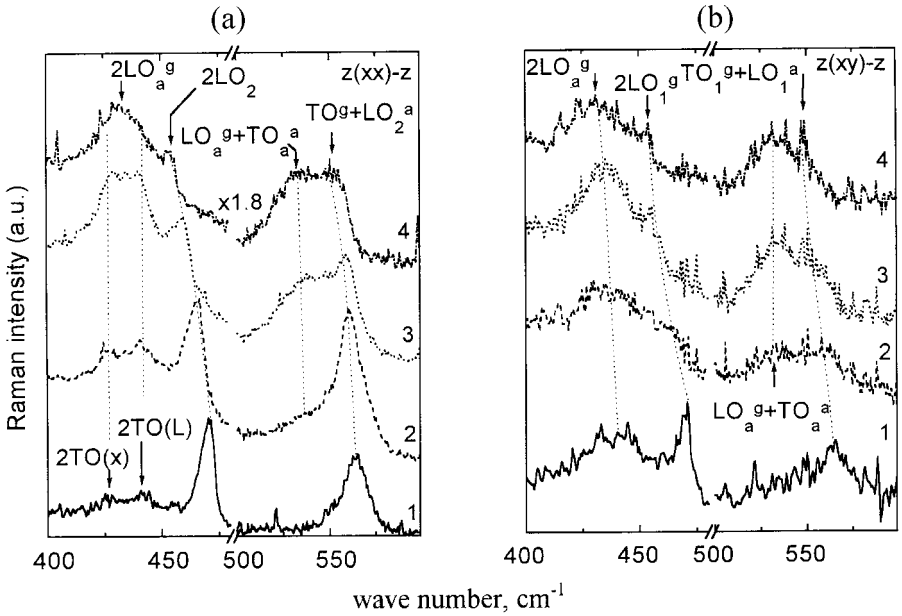

Fig. 7. The second-order Raman spectra of the $(GaSb)_n/(AlSb)_n$ superlattices measured for $z(xx)-z$ (a) and $z(xy)-z$ (b) scattering where $n = 10$ (curve 1), $n = 7$ (curve 2), $n = 4$ (curve 3), $n = 2$ (curve 4).

4 Conclusion

In conclusion we present an IR and Raman investigation on the optical vibrational spectrum of the GaSb/AlSb superlattices classified as SL with strained layers. The confinement of the optical phonons in the high-quality ultra-thin layer GaSb/AlSb superlattices with a thickness of the layers up to 2 ML was observed by IR and Raman spectroscopies. The dispersion of optical phonons of the GaSb and the AlSb obtained from analysis of the IR and Raman spectra is in a good accordance with the theoretical data and results of neutron and previous Raman scattering experiments. The analysis of IR and Raman data and the HRTEM experiments show that intermixing of atoms in the GaSb/AlSb SLs at the interface region of only 1–2 ML takes place that leads to a relaxation of the strain in the ultra-thin layer GaSb/AlSb SLs. The second-order Raman scattering spectra are dominated by overtones and combinations of the confined longitudinal and transverse optical GaSb and AlSb and GaSb-like and AlSb-like alloying modes which were identified also.

One of us (A.M.) acknowledge SMWK for financial support.

References

1. *Light Scattering in Solids V*, edited by M. Cardona, G. Güntherodt (Springer-Verlag, Berlin, 1989).
2. B. Lou, R. Sudharsanan, S. Perkowitz, Phys. Rev. B **38**, 2212 (1988).
3. Yu. Pusep, S.W. da Silva, J.C. Galzerani, A.G. Milekhin, V.V. Preobrazhenskii, B.R. Semyagin, I.I. Marahovka, Phys. Rev. B. **52**, 2610 (1995).
4. B. Samson, T. Dumelow, A.A. Hamilton, T.J. Parker, S.R.P. Smith, D.R. Tilley, C.T. Foxon, D. Hilton, K.J. Moore, Phys. Rev. B **46**, 2375 (1992).
5. C. Colvard, T.A. Gant, M.V. Klein, R. Merlin, R. Fisher, H. Morkoc, A.C. Gossard, Phys. Rev. B **31**, 2080 (1985).
6. G. Scamarcio, L. Tapfer, W. Konig, A. Fisher, K. Ploog, E. Molinari, S. Baroni, P. Giannozzi, S. de Gironcoli, Phys. Rev. B **43**, 14754 (1991).
7. Y. Ohmori, Y. Suzuki, H. Okamoto, Jpn J. Appl. Phys. **64**, 6733 (1988).
8. B. Jusserand, P. Voisin, M. Voos, L.L. Chang, E.E. Mendez, L. Esaki, Appl. Phys. Lett. **46**, 678 (1985).
9. G.P. Schwarz, G.J. Gualtieri, W.A. Sunder, L.A. Farrow, Phys. Rev. B **36**, 4868 (1987).
10. P.V. Santos, A.K. Sood, M. Cardona, K. Ploog, Y. Ohmori, H. Okamoto, Phys. Rev. B **37**, 6381 (1988).
11. D.W. Berreman, Phys. Rev. **130**, 2193 (1963).
12. B. Heinz, *Optische Konstanten von Halbleiter-Merschicht-Systemen*, Doctoral Dissertation, R.-W.T.H., Aachen (1991).
13. S.W. da Silva, Yu.A. Pusep, J.C. Galzerani, D.I. Lubyshev, A. Milekhin, V.V. Preobrazhenskii, M.A. Putiato, B.R. Semyagin, J. Appl. Phys. **80**, 597 (1996).
14. Y.S. Raptis, E. Anastassakis, G. Kanellis, Phys. Rev. B **46**, 15801 (1992).
15. M.P. Halsall, P. Dawson, J. Appl. Phys. **81**, 224 (1997).
16. M.K. Farr, J.G. Traylor, S.K. Sinha, Phys. Rev. B **11**, 1587 (1975).
17. D. Strauch, B. Dorner, K. Karch, in *Proceedings of the Third International Conference on Phonon Physics*, edited by S. Hunklinger, W. Ludwig (Heidelberg, 1989); *the Sixth International Conference on Phonon Scattering in Condensed Matter*, edited by G. Weiss (World Scientific, Singapore, 1990), p. 82.
18. T. Sekine, K. Uchinokura, E. Matsuura, Solid State Commun. **18**, 1337 (1976).
19. R. Ferrini, M. Galli, G. Guizzetti, M. Patrini, A. Bossacchi, S. Franchi, R. Magnanini, Phys. Rev. B **56**, 7549 (1997).